

**Scale ratios in decaying quasi-geostrophic turbulence (\*)(\*\*)**

D. G. DRITSCHEL

*School of Mathematics, The University of St. Andrews  
North Haugh, St. Andrews KY16 9SS, Scotland UK*

(ricevuto il 18 Novembre 1998; approvato il 6 Maggio 1999)

**Summary.** — The fundamental nature of rapidly rotating, stably stratified (*i.e.* quasi-geostrophic) turbulence has been debated since Charney (CHARNEY J. G., *Geostrophic turbulence*, *J. Atmos. Sci.*, **28** (1971) 1087-1095) proposed an isotropic theory for it. That theory implies that the (total) energy is partitioned, in spectral space, equally between the  $x$ ,  $y$  and  $z$  wave number components after scaling  $z$  in the governing equations by Prandtl's ratio  $f/N$ , or the ratio of the rotational and buoyancy frequencies. In (scaled) physical space, this implies that structures, *i.e.* vortices, would have equal dimensions, *i.e.* they would be spheres on average. Recent numerical results (DRITSCHEL D. G., DE LA TORRE JUÁREZ M. and AMBAUM M. H. P., *The three-dimensional vortical nature of atmospheric and oceanic turbulent flows*, *Phys. Fluids*, **11** (1998) 1512-1520), obtained at exceptionally high resolution, have confirmed for the first time Charney's prediction that vertical- to horizontal-scale ratios in quasi-geostrophic turbulence are equal to  $f/N$ . These results were largely unanticipated because the simulations analysed in Dritschel, de la Torre Juárez and Ambaum (1998) began with two-dimensional, height-independent vortices, and previous numerical simulations (MCWILLIAMS J. C., WEISS J. B. and YAVNEH I., *Anisotropy and coherent vortex structures in planetary turbulence*, *Science*, **264** (1994) 410-413) showed the emergence of approximately two-dimensional vortices at late times from isotropic, three-dimensional initial conditions. One key difference between Dritschel, de la Torre Juárez and Ambaum (1998) and McWilliams *et al.*, 1994 is the vertical boundary conditions used; in the former rigid, isothermal boundaries were used, while in the latter periodic boundaries were used. This difference was explored in (DRITSCHEL D. G. and MACASKILL C., *The role of boundary conditions in the simulation of rotating, stratified turbulence*, submitted to *Fluid Dyn. Res.*, which revealed that periodic boundaries tend to suppress three-dimensional behaviour by constraining the range of interactions between vortices, all other things being equal. Using a sufficiently wide domain, for fixed domain height, eventually reduces this constraint, allowing continued, three-dimensional behaviour. Here, we re-examine quasi-geostrophic turbulence in vertically periodic boundaries, at times well before two-dimensional vortices might emerge. We focus specifically on the characteristic scale ratio of structures, and how

(\*) Paper presented at the International Workshop on "Vortex Dynamics in Geophysical Flows", Castro Marina (LE), Italy, 22-26 June 1998.

(\*\*) The author of this paper has agreed to not receive the proofs for correction.

it compares to that found for rigid, isothermal boundaries (Dritschel, de la Torre Juárez and Ambaum, 1998).

PACS 92.10.Lq – Turbulence and diffusion.

PACS 47.27 – Turbulent flows, convection, and heat transfer.

PACS 47.27.Gs – Isotropic turbulence; homogeneous turbulence.

PACS 01.30.Cc – Conference proceedings.

## 1. – Physical motivation

The small- to intermediate-scale motions in the oceans, the atmosphere and other planetary atmospheres are aptly described as turbulent. At these scales (at and below the Rossby radius of deformation  $L_R$ , *i.e.* about 50 km in the oceans and 1000 km in the atmosphere), the fluid motion is highly unsteady and energetic [1-3]. These turbulent motions are, however, highly anisotropic due to the shallowness of these fluid systems and the effects of rotation and stratification; that is, vertical scales are typically much smaller than horizontal scales, and to leading order the motion is layerwise two-dimensional (running parallel to stratification surfaces), with the motions of each “layer” coupled through rotation.

This turbulence gives rise to secondary circulations that are largely responsible for the meridional (north-south) transport of heat, mass, chemical and biological constituents [2-5]. Though the large-scale circulation of the oceans and the atmosphere has been “spun up” by external forcing, fundamentally by solar radiation, the actual level of this forcing is generally extremely weak. That is, the free, inertial motions are much stronger at any given moment than the forcing. The effect of the forcing is to spin up, over a long time scale, a circulation which is, however, dynamically unstable. This instability is an integral part of the observed circulation, for it creates small-scale (*e.g.*, 10–100 km scale in the oceans, 100–1000 km scale in the atmosphere) “eddies” or coherent vortices whose net effect is to greatly weaken the mean circulation (*i.e.* they reduce the upper atmospheric winds by roughly 50%). See [2, 6] for background and for further implications.

At these scales, quasi-geostrophic theory is thought to be a good approximation for the flow away from boundary layers, strong topographic features, convective activity, and the upper atmosphere (where gravity wave breaking takes place) [7-11]. Quasi-geostrophic (QG) theory embodies the basic elements of rotation and stratification in the simplest possible manner, allowing one to focus on the essential factors controlling rotating, stably stratified turbulence. The governing equations are derived from the full, primitive (hydrostatic) equations by an asymptotic expansion in three small quantities: 1) the height-width aspect ratio  $\delta = H/L$  of characteristic motions (constrained to be small due to the shallow geometry); 2) the Rossby number  $Ro$  or ratio of the normal component of the relative vorticity  $\zeta$  to the normal component of the background vorticity  $f = 2\Omega \sin \phi$ , where  $\Omega$  is the planetary rotation rate and  $\phi$  is the latitude; and 3) the Froude number  $Fr$  or the ratio of relative (horizontal) fluid speeds  $U$  to the wave speed associated with stratification  $c = NH$ , where  $N$  is the buoyancy frequency. Note, in the atmosphere,  $f/N \sim 10^{-2}$ , while in the oceans,  $f/N \sim 10^{-1}$ . The Rossby radius  $L_R$  is defined by  $NH/f$ , where  $H$  is a characteristic height scale of the fluid (*i.e.* the full depth of the oceans or a density scale height (about

7 km) in the atmosphere). Quasi-geostrophy requires  $\delta \ll 1$  and  $\text{Fr}^2 \ll \text{Ro} \ll 1$  (see, for instance, [12]).

To understand fundamental aspects of rotating, stably stratified turbulence, research has focused on the unforced, weakly dissipated system, even though actual oceanic and atmospheric turbulence is maintained by weak levels of forcing (in effect this maintains a permanently unstable “basic state” [2, 6]). This effort was led three decades ago by Charney [7], who sought to explain some of the observed characteristics of atmospheric turbulence through a proposed scaling theory for QG turbulence (hereafter QGT)—see [13] for a historical survey. Though density decreases approximately exponentially with height in the atmosphere, Charney neglected this on the assumption that the prevalent turbulent “structures” had depths that were small compared with the density scale height and used the Boussinesq QG equations, which are more appropriate for oceanic flows. For the same reason, he neglected the variation of the buoyancy frequency  $N$  with height. He also neglected the variation of the Coriolis parameter with latitude, assuming that the turbulent structures were of sufficiently small horizontal scale. With constant  $f$ ,  $N$ , and density, the governing equations then reduce to the simple form

$$(1a) \quad \frac{\partial q}{\partial t} + \mathbf{u} \cdot \nabla q \equiv \frac{Dq}{Dt} = 0,$$

$$(1b) \quad \nabla^2 \psi = q,$$

$$(1c, d) \quad u = -\frac{\partial \psi}{\partial y} \quad \text{and} \quad v = \frac{\partial \psi}{\partial x},$$

*i.e.* one equation for the (horizontal) advection or conservation of potential vorticity  $q$ , and a linear inversion relation giving the velocity field  $(u(x, y, z, t), v(x, y, z, t), 0)$  in terms of the potential vorticity (PV). Here, the  $z$  coordinate has been scaled by  $f/N$  so that  $\nabla^2$  is the three-dimensional Laplacian operator. Notably, the entire nonlinearity of this system lies in the advection of PV. Also, the relation between the streamfunction  $\psi$  and the PV  $q$  is isotropic, but the velocity field is completely anisotropic—it has no vertical component (to this order in the asymptotic expansion).

The most significant prediction made by Charney was that the energy spectrum should be isotropic, despite the velocity field anisotropy. In fact, he came to this conclusion after having exhausted all possible scales; however, and this appears to be significant, the absence of vertical motion does not introduce new scales and therefore cannot be used in a scaling theory. The isotropy of QG turbulence remains an open question; the results of ref. [13] only verify a prediction of Charney’s theory, namely that vertical- to horizontal-scale ratios are equal to  $f/N$ . Charney also claimed that the energy spectrum  $\mathcal{E}(k) \sim k^{-3}$ , where  $k$  is the magnitude of the 3D wave number after scaling  $k_z$  by  $N/f$ , and this *together with* isotropy implies that vertical- to horizontal-scale ratios, as defined below, are equal to  $f/N$ .

The results of [13] were obtained for QGT bounded at  $z = 0$  and  $H$  by rigid, isothermal boundaries (at which  $\partial\psi/\partial z = 0$ ) and laterally by periodic walls. In this paper, we examine results obtained for vertically periodic boundaries. As in previous work [14], an isotropic domain having equal side lengths is considered. Section 2 describes the results of two exceptionally high-resolution simulations that were conducted using the same numerical method employed in [13]. The form of the PV field

at late times is examined, and the vertical to horizontal scale ratios are quantified. The differences between the results obtained for the two types of vertical boundaries are discussed in sect. 3.

## 2. – Simulation results

**2.1. The numerical method.** – The simulations described below were conducted using the new “Contour-Advection Semi-Lagrangian” (CASL) algorithm [15]. This algorithm represents the PV field as a set of contours (or isolevels) as in contour dynamics and carries out PV advection (the solution of eq.(1a)) by solving the equivalent equation  $d\mathbf{x}/dt = \mathbf{u}(\mathbf{x}, t)$  for each  $\mathbf{x}$  on each contour. Unlike contour dynamics, the velocity field is obtained by conventional methods, here spectrally. This “inversion” problem is linear and is efficiently solved in this manner. The gridded PV field needed for this is obtained by a fast domain-filling procedure described in [15]. The result is a gridded velocity field, which is interpolated to the points  $\mathbf{x}$  on each contour, permitting one to integrate the system forward in time. Dissipation of PV occurs by way of “surgery”, which removes exclusively filamentary PV at one-tenth of the basic grid scale used to carry out the inversion. This non-diffusive dissipation results in much better PV conservation compared to the dissipation required by conventional grid-based methods (*e.g.*, hyperviscosity in the case of the pseudo-spectral method)—see [16]. As to performance, refs. [15,16] demonstrate that this hybrid algorithm is typically 1000 times faster than either the pseudo-spectral or the contour-dynamics method.

**2.2. Flow initialization.** – The two simulations conducted were initialised by  $N$  identical spherical volumes of uniform PV, one half having  $q = +Q$  and the other half having  $q = -Q$ , randomly distributed throughout the domain. This is the simplest possible isotropic prescription of the PV field, and it allows comparison with the results of [2] (for rigid vertical boundary conditions). A variety of prescriptions however should be studied before drawing universal conclusions. Initially, a fraction  $F$  of the volume contains non-zero PV, and the minimum inter-vortex separation was  $d_{\min}$  (always greater than  $2R$ , where  $R$  is the vortex radius, to prevent overlapping). The PV was arbitrarily chosen to be  $4\pi$  to make one unit of time equal to a “vortex rotation period” (this at least is the time a cylindrical column would take to rotate once). For accurate advection, a time step of  $1/40$  has been used [15,16].

The two simulations,  $\mathcal{A}$  and  $\mathcal{B}$ , have the following initial characteristics:

$$\begin{aligned} \mathcal{A} : N = 400, \quad F = 0.05, \quad d_{\min} = 4R \text{ and } n_g = 256, \\ \mathcal{B} : N = 200, \quad F = 0.20, \quad d_{\min} = 2R \text{ and } n_g = 128, \end{aligned}$$

where  $n_g$  is the grid resolution used to obtain the velocity field. The volume fraction  $F$  may appear to be small, but in fact  $F = 0.05$  or smaller is typical of the late-time PV field according to previous work [13,14]. In time, vortex interactions generate a down-scale cascade of PV leaving progressively less coherent PV. This is particularly true here of simulation  $\mathcal{B}$ ; moderate  $F$  values permit very strong vortex interactions and a rapid down-scale cascade of PV, so that after only a few tens of time units (vortex rotation periods), the coherent volume fraction has diminished to around  $F = 0.05$ .

**2.3. Vortex characteristics.** – Here, we examine qualitatively the evolution of the PV field in simulation  $\mathcal{A}$ . Simulation  $\mathcal{B}$  is not significantly different once it enters the decaying stage of evolution. Both simulations exhibit a rapid growth in complexity, but this is especially notable in simulation  $\mathcal{B}$ , where the number of points representing the PV contours climbs from 150324 at  $t=0$  to a maximum of 1172011 by  $t=12$ . By comparison, in simulation  $\mathcal{A}$ , the number of points climbs from 147310 at  $t=0$  to a maximum of 700003 by  $t=34$ . This initial growth in complexity occurs because the initial PV field is quite unlike that found during the decaying stage (after the peak in complexity), when vortex interactions are far less numerous. The vortices appear to become distributed in size and space to minimise interactions with one another (for a related hypothesis, see [17]).

Figure 1 shows simulation  $\mathcal{A}$  at four times,  $t=0$ ,  $t=40$ ,  $t=100$  and  $t=250$ . At  $t=40$ , the abundant filamentary PV obscures much of the coherent PV field. At the two later times, one sees the emergent PV structures, no longer perfectly spherical of course, but not greatly differing from this shape. Note the wide distribution of vortex volumes present at these times (the form of this distribution has not yet been

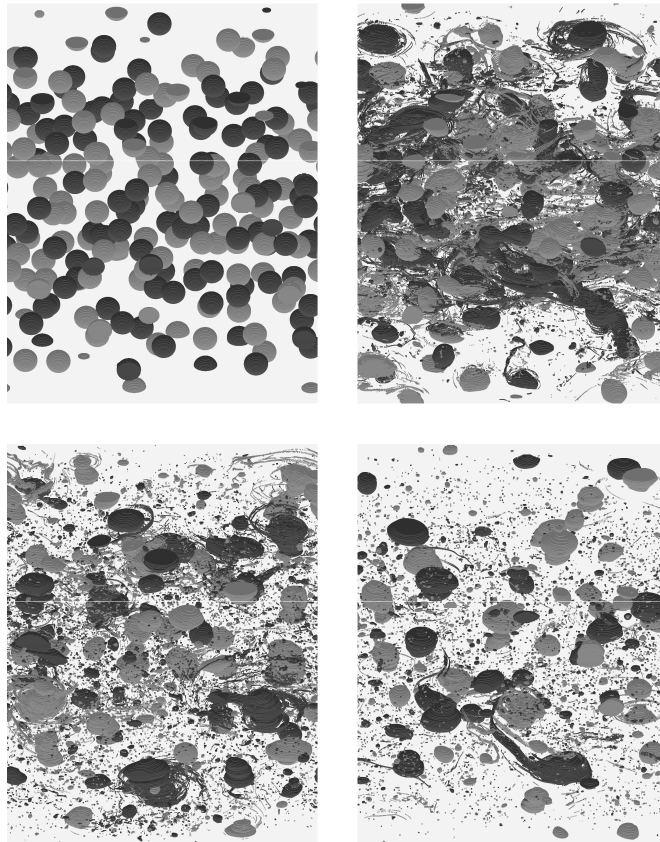


Fig. 1. – Images of the PV field in simulation  $\mathcal{A}$  at times  $t=0$  (top left),  $t=40$  (top right),  $t=100$  (bottom left) and  $t=250$  (bottom right). Positive PV is rendered a darker shade of grey than negative PV. The flow is viewed from an infinite vantage point in the plane  $x=0$  at an angle of  $60^\circ$  from the vertical.

quantified). The volume fraction of PV at these times is 0.05, 0.0419, 0.0288, and 0.0200—it decreases most slowly between  $t = 100$  and 250 when vortex interactions are relatively infrequent.

**2.4. Spectral partition.** – Two time periods from each simulation are next analysed following [13] to determine the partition of energy between the horizontal and vertical wave number components. The procedure consists in calculating the 1D *horizontal* energy spectrum  $E_m(K)$  for each vertical wave number  $m$ , with  $m$  ranging from 0 to  $n_g/2 - 1$  (the computational box has a side length of  $2\pi$  in each direction). Each horizontal wave number,  $k_x$  and  $k_y$ , similarly ranges from 0 to  $n_g/2 - 1$ , and  $K$  is defined by  $K \equiv \sqrt{k_x^2 + k_y^2}$ . As usual, the 2D spectrum  $E_m(k_x, k_y)$  is binned according to the nearest integer value of  $K$  to form the 1D spectrum  $E_m(K)$ , in which  $K$  is now regarded as an integer. The sum of  $E_m$  over all  $K$  gives the total energy for each vertical wave number  $m$ , and the sum of these sums gives the total energy, which is conserved in theory. The next step is to calculate the mean horizontal wave number  $\bar{K}_m$  for each  $m$  from  $\bar{K}_m = \sum_K K E_m(K) / \sum_K E_m(K)$ . The dependence of  $\bar{K}_m$  on  $m$  was used in [13] as a measure of isotropy; there  $\bar{K}_m \approx m$  was found at late times (for rigid vertical boundary conditions).

The present results, for periodic boundary conditions, are given in fig. 2 at two times for each simulation; the solid lines show the results for simulation  $\mathcal{A}$  averaged over  $110 \leq t \leq 130$  (21 samples; thin line) and over  $240 \leq t \leq 260$  (bold line), while the dashed lines show the results for simulation  $\mathcal{B}$  over  $90 \leq t \leq 110$  (short-dashed) and  $290 \leq t \leq 310$  (long-dashed). As discussed in [13], the calculation of  $\bar{K}_m$  does not appear to be reliable for  $m$  exceeding half the maximum wave number, which is 32 for simulation  $\mathcal{B}$ . This is seen in fig. 2 (dashed curves) which bends up at high  $m$ .

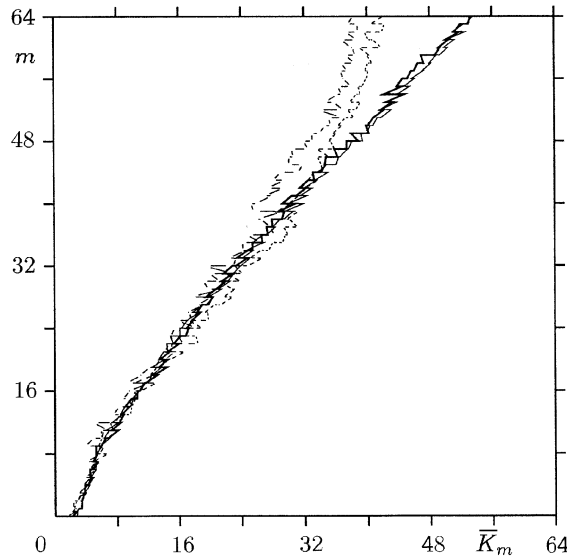


Fig. 2. – The dependence of the mean horizontal wave number  $\bar{K}_m$  (abscissa) on the vertical wave number  $m$  (ordinate); the short- and long-dashed curves are for simulation  $\mathcal{B}$  averaged over  $90 \leq t \leq 110$  and over  $290 \leq t \leq 310$ , while the thin and bold solid curves are for simulation  $\mathcal{A}$  averaged over  $110 \leq t \leq 130$  and over  $240 \leq t \leq 260$ .

Simulation  $\mathcal{A}$ , on the other hand, has a maximum wave number of 128 (in each direction), and one can see that, up to  $m = 64$ , the curve  $\bar{K}_m$  vs.  $m$  is approximately a straight line apart from near the very lowest values of  $m$ , as found also in [13]. A least-squares fit to the straight line  $\bar{K}_m = \alpha + \beta m$  for  $8 \leq m \leq 64$  gives  $\beta = 0.883 \pm 0.028$  for  $110 \leq t \leq 130$  and  $\beta = 0.858 \pm 0.030$  for  $240 \leq t \leq 260$  (N.B.: the corresponding intercepts,  $\alpha$ , are  $-3.8$  and  $-3.2$ , respectively). The slope  $\beta$  varies little during this late period of the simulation, and maintains a value significantly different from unity.

### 3. – Discussion

In QGT between rigid, isothermal boundaries, a slope of unity was found between the horizontal and vertical wave numbers for all but the lowest wave numbers. Here, for vertically periodic boundaries, a slope slightly less than unity is observed. The simulations conducted for the two different boundary conditions differ also in other respects; here the domain is a cube (after scaling  $z$  by  $f/N$ ), whereas in ref. [13] the domain is shallow (one-sixteenth of its width); moreover, here the flow is initialised with spherical volumes of PV, whereas in ref. [13] it is initialised with columnar vortices. Therefore, it is premature to conclude that the observed differences are attributable to the boundary conditions alone. What is clear is that a systematic study is needed to come to a basic understanding of rotating, stably stratified turbulence. A wide range of initial conditions, domain shapes, and boundary conditions needs to be explored, and this will require extensive numerical simulation. Fortunately, the CASL algorithm has brought this goal within reach.

\* \* \*

DGD is supported by the UK Natural Environment Research Council.

### REFERENCES

- [1] GAGE K. S. and NASTROM G. D., *On the spectrum of atmospheric velocity fluctuations seen by MST/ST radar and their interpretation*, *Radio Science*, **20** (1985) 1339-1347.
- [2] HOLTON J. R., HAYNES P. H., MCINTYRE M. E., DOUGLASS A. R., ROOD R. B. and PFISTER L., *Stratosphere-troposphere exchange*, *Rev. Geophys.*, **33** (1995) 403-439.
- [3] WUNSCH C. and STAMMER D., *The global frequency-wavenumber spectrum of oceanic variability estimated from TOPEX/POSEIDON altimetric measurements*, *J. Geophys. Res. C*, **100** (1996) 24895-24910.
- [4] RHINES P. B. and YOUNG W. R., *Homogenization of potential vorticity in planetary gyres*, *J. Fluid Mech.*, **122** (1982) 347-367.
- [5] HOLLAND W. R. and MCWILLIAMS J. C., *Computer modeling in physical oceanography: from the global circulation to turbulence*, *Phys. Today*, **40** (1987) 51-57.
- [6] AMBAUM M. H. P., *Isentropic formation of the tropopause*, *J. Atmos. Sci.*, **54** (1997) 555-568.
- [7] CHARNEY J. G., *Geostrophic turbulence*, *J. Atmos. Sci.*, **28** (1971) 1087-1095.
- [8] SIMMONS A. J. and HOSKINS B. J., *Baroclinic instability on the sphere: Normal modes of the primitive and quasi-geostrophic equations*, *J. Atmos. Sci.*, **33** (1976) 1454-1477.
- [9] GILL A. E., *Atmosphere-Ocean Dynamics* (Academic Press) 1982.
- [10] HOLTON J. R., *An introduction to dynamic meteorology* (Academic Press Inc., San Diego) 1982.

- [11] HOSKINS B. J., MCINTYRE M. E. and ROBERTSON A. W., *On the use and significance of isentropic potential-vorticity maps*, *Q. J. R. Meteorol. Soc.*, **111** (1985) 877-946.
- [12] STEGNER A. and ZEITLIN V., *What can asymptotic expansions tell us about large-scale quasi-geostrophic anticyclonic vortices?* *Nonlin. Processes Geophys.*, **2** (1995) 186.
- [13] DRITSCHER D. G., DE LA TORRE JUÁREZ M. and AMBAUM M. H. P., *The three-dimensional vortical nature of atmospheric and oceanic turbulent flows*, *Phys. Fluids*, **11** (1998) 1512-1520.
- [14] MCWILLIAMS J. C., WEISS J. B. and YAVNEH I., *Anisotropy and coherent vortex structures in planetary turbulence*, *Science*, **264** (1994) 410-413.
- [15] DRITSCHER D. G. and AMBAUM M. H. P., *A contour-advective semi-Lagrangian algorithm for the simulation of fine-scale conservative fields*, *Q. J. R. Meteorol. Soc.*, **123** (1997) 1097-1130.
- [16] DRITSCHER D. G., POLVANI L. M. and MOHEBALHOJEH A. R., *The contour-advective semi-Lagrangian algorithm for the shallow-water equations*, *Mon. Weath. Rev.*, **127** (1998) 1151-1165.
- [17] DRITSCHER D. G., *Vortex properties of two-dimensional turbulence*, *Phys. Fluids A*, **5** (1993) 984-997.